

GPO PRICE \$ _____

CFSTI PRICE(S) \$ _____

Hard copy (HC) 1

Microfiche (MF)

ff 653 July 65

VACUUM HOT-PRESSING OF MAGNESIUM ALUMINATE


By Donald R. Rummel

NASA Langley Research Center
Langley Station, Hampton, Va.

Presented at the American Ceramic Society,
Basic Science Division Meeting

FACILITY FORM 602	<u>N 68-27461</u> (ACCESSION NUMBER)	<u> </u> (THRU)
	<u>41</u> (PAGES)	<u>1</u> (CODE)
	<u>TMX-59053</u> (NASA CR OR TMX OR AD NUMBER)	<u>15</u> (CATEGORY)

University Park, Pennsylvania
October 9-11, 1966



VACUUM HOT-PRESSING OF MAGNESIUM ALUMINATE


By Donald R. Rummel

SUMMARY

The purposes of this investigation were to (1) examine the applicability of a phenomenological rate equation for hot-pressing and (2) characterize the densification behavior of magnesium aluminate during hot-pressing. In order to accomplish these objectives, the densification kinetics of magnesium aluminate powder compacts during vacuum hot-pressing were studied between 1175° and 1460° C and from 500 to 5100 psi.

The proposed rate equation, which treats porosity as a functionally independent variable, is analogous to several relationships which have been proposed for unconstrained creep. It is shown that the treatment of porosity as an independent variable is reasonable and does not functionally restrict porosity as a modifier of the applied stress.

Below 1350° C the densification characteristics of magnesium aluminate were similar to those reported for other oxide systems. Above 1350° C neither diffusional creep nor plastic flow models for hot-pressing adequately described the densification behavior observed. The rate equation, which suggests a logarithmic relationship between strain rate and porosity, provided an excellent description of the observed densification. The strain rate dependence on porosity was found to decrease at a porosity of approximately 0.15. The observed change in porosity dependence was not strongly influenced by stress or temperature.



Between 1350° and 1450° C the apparent activation energy for densification was found to be stress dependent. At 1450° C an increase in the stress dependence of the densification rate and an interaction between stress and porosity indicated that plastic flow by dislocation motion was probably an operative mechanism during densification.

INTRODUCTION

Recently there has been increased interest in magnesium aluminate ($MgAl_2O_4$) as a possible candidate material for high temperature structural applications. In addition to being chemically and thermally stable, magnesium aluminate (spinel) is isotropic and possesses the multiplicity of slip systems which are necessary for generalized plastic deformation in a polycrystalline body. Although spinel has a potential for ductile behavior at elevated temperature, its structural performance is highly sensitive to the same microstructural variables which affect other ceramic materials; i.e., porosity and grain size. The desire to control both porosity and grain size has led to the current interest in hot-pressing as a fabrication process for ceramic materials. Hot-pressing makes possible the fabrication of powder compacts which have low porosity and small grain size, both desirable microstructural features.

Unfortunately the mechanism or mechanisms which control densification during hot-pressing are not explicitly understood. Plastic flow (refs. 1 and 2) and stress-enhanced volume diffusion (refs. 3 and 4) have both been suggested as material transport mechanisms during the final stages of densification. A relationship which combines plastic flow and diffusion

models and includes the consideration of grain growth during hot-pressing has also been suggested (ref. 5). Although these models stem from consideration of different phenomena, they all predict a linear relationship between the rate of densification and the applied stress. In addition they all consider porosity as the dependent variable.

Recently a phenomenological rate equation for hot-pressing has been suggested by Kriegel, Palmour, and Choi (ref. 6). The rate equation treats porosity as a functionally independent variable and is analogous to several relationships which have been proposed for unconstrained creep. In addition, it does not exclude a nonlinear densification rate-stress dependency.

The purposes of this investigation were to (1) characterize the densification behavior of magnesium aluminate during vacuum hot-pressing and (2) examine the applicability of the phenomenological rate equation for hot-pressing proposed by Kriegel, et al. In order to accomplish these objectives, the densification kinetics of magnesium aluminate powder compacts were studied by vacuum hot-pressing between 1175° and 1460° C and from 500 to 5100 psi.

SYMBOLS

A	experimentally determined constant
b_0	multiple regression intercept
B, C	constants
D	relative density
e	strain based on original compact height

$\dot{\epsilon}$	$\frac{d\epsilon}{dt}, \text{ min}^{-1}$
k	$\log_{10} 2.718 = 0.4343$
K	densification rate constant
m	experimentally determined porosity exponent
n	experimentally determined stress exponent
P	instantaneous volume fraction porosity
P_0	initial volume fraction porosity
Q	apparent activation energy for densification, cal/mole
R	universal gas constant, 1.986 cal/°K
t	time, minutes
T	temperature, °K
α, β	porosity exponent constants
ϵ	strain based on instantaneous height
$\dot{\epsilon}$	$\frac{d\epsilon}{dt}, \text{ min}^{-1}$
σ	normal applied stress, psi
σ_e	effective stress, psi
Subscript	
av	average

PROCEDURE

Material

The fine grain ($\approx 0.3\mu$) magnesium aluminate used in this investigation was approximately 98.5 percent pure with a slight excess of magnesia

(MgO:Al₂O₃ ≈ 1.1). The powder was prepared by reacting alumina trihydrate and magnesium hydroxide in the presence of aluminum fluoride (ref. 7) and was obtained from Aluminum Laboratories Limited, Box 250, Arvida, P. Q., Canada.

Apparatus

A vacuum furnace and graphite punches and dies in conjunction with a screw-powered universal testing machine were utilized for hot-pressing. The furnace had a tungsten mesh resistance heating element and metallic heat shields. The furnace pumping system maintained the chamber pressure below 5×10^{-3} torr during all experiments. A tantalum shielded tungsten - 5 percent rhenium/tungsten - 26 percent rhenium thermocouple in close proximity to the hot-pressing die was used to control temperature. Because of the long-term instability of tungsten based thermocouples, the reported pressing temperatures were determined with a micro-optical pyrometer sighted on the graphite die body. Temperature differences between the exterior and interior walls of the graphite die and temperature variation of the die wall exterior in the vicinity of the compact were found to be insignificant after equilibrium had been established. The pressing loads were transmitted to the graphite punches by water-cooled stainless steel push rods. These rods were sealed by metallic bellows and rigidly attached to the platens of the 10,000 pound capacity universal screw-powered testing machine. The bellows spring constant was found to be negligible. The die was unrestrained in order to achieve double-acting punch response.

The displacement of the moving punch was sensed by a linear variable differential transformer (LVDT) and continuously recorded on a modified strip chart recorder. The chart paper advance, normally the time axis of the recorder, responded to the output signal of the LVDT. The displacement recording system was found to be linear throughout the 0.2-inch range of the LVDT and capable of detecting a displacement of 5×10^{-5} inches. The punch load was recorded on the other axis of the recorder. A timing mark was electrically superimposed on the load axis every minute.

The dies (2 inches O.D. and 0.5 inch I.D.) and punches were machined from dense, fine-grain, low-ash graphite. A loose sliding fit was established between the punches and die to allow removal of residual gases in the spinel powder during hot-pressing. Thin (0.01 inch) graphite spacers were used to separate the punch faces from the spinel powder and to protect the punch faces from the minor surface reaction which was observed at the higher pressing temperatures.

Hot-Pressing Procedure

The graphite die was charged with 3.60 g of dry spinel powder and the powder slowly cold-pressed to 1500 psi. The die assembly was inverted, and the powder was recompactd to 3000 psi. After cold-pressing, the compacts were approximately 50 percent of theoretical density (assumed to be 3.584 g/cm^3). The die assembly was inserted between push rods and a small preload applied. The furnace chamber was evacuated and the load indicator rezeroed to the applied preload to correct for the influence of

atmospheric pressure on the moving punch. The full test pressure was applied to the compact before heating the die. After reaching the test temperature, the furnace controller was switched to the automatic mode and the punch displacement measuring system zeroed. The applied load was maintained within ± 1 percent throughout each experiment by manually controlling the punch displacement rate.

Bulk Density Determination

The bulk density of the hot-pressed specimens was determined by water immersion techniques. Following cold extraction from the graphite die, the ends of the specimens were lightly sanded on 80 grit silicon carbide paper to remove rough edges and flatten the surfaces for height measurements. To remove surface graphite the specimens were oxidized at 750° C in air for 24 hours and cooled in a desiccator. Reproducible bulk density determinations could not be made using standard water immersion techniques; consequently, the specimens were given a wash coat of cellulose nitrate to preclude water penetration. The reported bulk densities include a correction for the volume of the wash coat which was typically 0.005 cm³. The standard error of the bulk density determinations was found to be less than 0.05 percent, and the systematic errors are estimated to be less than 0.05 percent.

Data Reduction

From the final density and height of a compact and the time-displacement record, the relative density of a compact at any time was calculated. The use

of true strain is necessary when considering processes which result in considerable deformation; consequently, the instantaneous strain rate of a compact was calculated as follows:

$$\dot{\epsilon} = - \frac{dh}{hdt}$$

which is equivalent to

$$\dot{\epsilon} = \frac{dD}{Ddt}$$

where a decrease in height is assumed to result in a positive strain. The resulting densification data for each compact were then fitted by the method of least squares to an equation of the following form:

$$\log \dot{\epsilon} = \log C + m \log P$$

where

P = instantaneous volume fraction porosity

C = constant

Although variations between the actual and nominal test temperatures occurred, all graphical presentations of the data are made at the nominal test temperature.

RESULTS

Final Compact Bulk Density

The major processing parameters and the resultant bulk density and porosity for the vacuum hot-pressed spinel compacts fabricated during this investigation are presented in table I. The following observations can be made from this table:

1. Spinel can be vacuum hot-pressed to near theoretical density at temperatures as low as 1300° C, with pressures as low as 2500 psi.
2. When hot-pressed under similar conditions, the bulk density of compacts was reproducible (see, for example, 24, 25, 26, and 27).
3. The final density of the compacts was not strongly dependent on the time required to reach the pressing temperature (see, for example, 21 and 22).
4. At moderate temperatures, even at porosities of less than 0.01, additional pressing time produced a measurable decrease in porosity (see, for example, compacts 32 and 33).
5. When compacts were fabricated at the higher temperatures and pressures there was some indication of an end-point porosity (see, for example, 42 and 43).
6. At temperatures below 1260° C no appreciable densification of the spinel compacts was evident after pressing for as long as 300 minutes (see, for example, 1, 5, 6, and 8).

Densification Kinetics

The final stage densification kinetics of oxide systems (see, for example, refs. 8, 9, 10) and systems which have liquid phase (ref. 11) have been found to be in agreement with the plastic flow model suggested by Murray, et al (ref. 1) which in its integral form predicts a linear relationship between log porosity and time. For constant grain size, this relationship also describes densification by diffusional creep (ref. 4).

Typical hot-pressing kinetics for the spinel compacts in this investigation are shown in figure 1. Below 1350° C the densification kinetics of the spinel compacts are in general agreement with the kinetics of the Murray expression. At temperatures of 1350° C and above, however, the densification behavior of the spinel compacts suggests a change in the mechanism and/or mechanisms which control densification. A plot of densification rate versus porosity (fig. 2) indicates that with the possible exception of the data at 1450° C the extrapolated data intersected the origin. The absence of an end-point density is indicative of a diffusionally controlled process (ref. 3). If densification is controlled by a diffusional creep mechanism (refs. 12 and 13), then consideration of the grain growth which may occur during densification is appropriate. A relationship for hot-pressing which considers grain growth has been proposed by Kovaltschenko and Samsonov (ref. 5). These authors substituted the expression for coefficient of viscosity developed for diffusional creep (refs. 12 and 13) and the parabolic relationship for normal grain growth into the Murray equation. The integral form of the resulting expression was hyperbolic and predicted a linear relationship between log porosity and log time. General agreement with this expression has been observed for tantalum carbide (ref. 14), lead (ref. 15), tin (ref. 15) and sodium chloride-water compacts (ref. 11). The densification behavior of the spinel compacts (fig. 3) at 1350° C and above was also in general agreement with the hyperbolic expression. This agreement would suggest that the deviation from the Murray expression above 1350° C was due to the effects of grain growth rather than a change in the controlling densification mechanism.

In summary, the densification behavior of the spinel compacts could not be adequately characterized by any single densification model for hot-pressing.

ANALYSIS AND DISCUSSION

In the following two sections a densification rate equation is presented, its implications discussed, and its applicability demonstrated. The densification behavior of the spinel compacts in this investigation is then characterized in terms of the rate equation.

Development of Rate Equation

One of the major objectives of this investigation was to evaluate the applicability of the phenomenological rate equation proposed for hot-pressing by Kriegel, Palmour, and Choi (ref. 6):

$$\dot{e} = A (P_0 - e)^m \sigma^n \exp \left(-\frac{Q}{RT} \right) \quad (1)$$

e = strain based on original compact height

$$\dot{e} = \frac{de}{dt}$$

σ = applied normal stress

P_0 = initial volume fraction porosity

Q = apparent activation energy for densification

T = temperature in °K

R = universal gas constant

A , m , and n = experimentally determined constants

Recognizing that $(P_0 - e)$ is equivalent to the instantaneous volume fraction porosity and that the use of true strain is necessary for processes which involve considerable deformation, equation (1) takes the following form at constant temperature:

$$\dot{\epsilon} = B \sigma^n P^m \quad (2)$$

$\dot{\epsilon}$ = strain rate based on instantaneous compact height

$$B = A \exp\left(-\frac{Q}{RT}\right)$$

P = instantaneous volume fraction porosity

It is appropriate to examine the implications of equation (2), particularly in view of the fact that porosity is treated as an independent variable in contrast to other hot-pressing relationships (refs. 2 and 4) which consider porosity as a modifier of the stress which is effective during pore closure. Porosity reduces the cross-sectional area of material transferring load and as a consequence several relationships (see, for example, refs. 2, 17, and 18) have been proposed to calculate an effective stress in terms of the applied stress and the volume fraction porosity. It can be demonstrated that these relationships are adequately represented at low porosities ($P \leq .15$) by

$$\sigma_e = C \sigma P^\alpha \quad (3)$$

where σ_e is the effective stress and C and α are constants. As an alternate to equation (2), porosity and stress can now be considered interrelated

$$\dot{\epsilon} = K (\sigma P^\alpha)^n \quad (4)$$

where K is a constant at any temperature. The similarity between equations

2 and 4 is obvious. The treatment of porosity as an independent variable is therefore reasonable and does not functionally restrict porosity as a modifier of the applied stress since equation (4) can be modified

$$\dot{\epsilon} = K (\sigma P^\alpha)^n P^\beta \quad (5)$$

so that $(n\alpha + \beta) = (m)$ in equation 2.

It is of interest to note that for $m \approx 1.1$ and $n \approx 1.0$ equation (5) reduces to

$$\frac{dD}{dt} = K \sigma_e (P - P^2) \quad (6)$$

where D = relative density. Assuming the squared term to be negligible for low values of porosity, equation (6) yields

$$\frac{dD}{dt} = K \sigma_e (1 - D) \quad (7)$$

which is in general agreement with the kinetics suggested for the plastic flow model of Murray, et al (ref. 1) and the diffusional creep expression proposed by Rossi and Fulrath (ref. 4).

The rate equation (2) suggests a logarithmic relationship between the true strain rate and porosity. The applicability of this relationship is shown in figure 4. The solid lines represent the best fit (method of least squares) of the data for each test. Even at the higher test temperatures, the rate equation appears to adequately predict the densification kinetics observed. The equation does not, however, suggest the change in slope which was observed in the test at 1260° C at approximately 0.15 porosity. The densification data from other tests which include both regimes (fig. 5)

confirm that the change in slope at approximately $P = 0.15$ is a function of porosity and is not strongly influenced by temperature or pressure.

Densification Characterization

In the following subsections, the densification kinetics which were observed in this investigation will be examined using the logarithmic form of the rate equation (2)

$$\log \dot{\epsilon} = \log A + m \log P + n \log \sigma - k \frac{Q}{RT} \quad (8)$$

where $k = 0.4343$.

Porosity dependence.— The results of the linear regression on

$$\log \dot{\epsilon} = \log C + m \log P \quad (9)$$

are presented in table I for each compact. This table also presents the correlation coefficient, the degrees of freedom, and the calculated values of porosity for a strain rate of 0.01/minute and 0.0001/minute for each regression. For the reader who is unfamiliar with statistical terminology, the square of the correlation coefficient is equal to the fraction of the strain rate variance which is accounted for by the regression line and the degrees of freedom are equal to $(N - 2)$ where N is the number of observations of strain rate and porosity included in the regression line.

For compacts which included both hot-pressing regimes, the fitted data include only the low porosity regime ($P \leq 0.15$). Porosity was calculated for strain rates of 0.01/minute and 0.0001/minute for each compact to facilitate comparison of the regression results. For some

compacts these calculated porosities represent an extrapolation of the densification data.

The following observations can be made from table I.

1. The high correlation coefficients indicate that the regression equation adequately describes the densification kinetics which were observed.

2. In the high porosity regime at temperatures below 1275° C, longer pressing time and/or lower final compact porosity reduced both the slope (m) and intercept (log C) of the regression lines.

3. Between 1275 and 1390° C, in the low porosity regime, the slopes of the regression lines appear to be independent of temperature, stress, pressing time, and final porosity.

4. Above 1390° C there is an increase in the slopes of the regression lines.

5. In the low porosity regime the intercept of the regression lines (log C) generally decreases with increasing stress.

In figures 6, 7, and 8, average regression lines for given applied stresses are presented for several test temperatures. Although there was limited densification observed at 1220° C, the regression lines (fig. 6) did show that an increase in stress increased the observed strain rate for any given porosity and that porosity was not independent of stress since the regression lines are not parallel. The steep slope (large value for m) indicates that complete densification will occur slowly, if at all.

The average regression lines in the low porosity regime are presented for the 1350° C tests in figure 7. This figure illustrates the following: (1) the slope (value of m) is approximately one, (2) an increase in the

applied stress increases the strain rate at any given porosity, and (3) an interaction term involving porosity and stress is not required to fit the data since the lines are approximately parallel. Similar kinetics were observed for the compacts hot-pressed at 1300° and 1390° C.

At 1450° C the slopes of the regression lines at 867 and 1500 psi (fig. 8) were approximately one and did not indicate any interaction between stress and porosity. Above 1500 psi, however, the regression lines are not parallel and an interaction between stress and porosity is clearly indicated. The intersection of the 1500 psi regression line with those at higher stresses indicates that the previously mentioned end-point porosity was probably the result of pore entrapment rather than failure to exceed the critical shear stress of a Bingham solid (ref. 2).

The average value of the porosity exponent (m) at 1450° C was found to be linearly dependent on stress. This linear dependency is shown in figure 9 which also illustrates the stress independence of (m) at 1350° C. The stress dependence of the porosity exponent is inconsistent with the consideration of porosity solely as an indicator of the compact inter-particle contact area, which at a given porosity would be independent of stress.

Stress dependence.— The stress dependence of the strain rate at 1350° C was essentially linear (fig. 10) and was not strongly influenced by porosity. Linear dependence of strain rate on stress was also observed at 1300° C and 1390° C. The stress dependence of strain rate at 1450° C (fig. 11) was linear to 2500 psi for 0.05 porosity and to 3500 psi for 0.05 porosity. Above these stresses the value of (n) increased and in the case

of 0.05 porosity the (n) value increased to approximately four suggesting a change in the mechanism controlling densification. A similar change in stress dependency in the creep behavior of aluminum (ref. 19) has been attributed to a change in mechanism from one of bulk diffusion (refs. 12 and 13) to one of dislocation climb proposed by Weertman (ref. 20). The present data are consistent with other investigations (refs. 21, 22, and 23) which indicate general agreement with the Weertman analysis ($\dot{\epsilon} \approx \sigma^4$) for spinel at temperatures above 1350° C.

Temperature dependence.— The temperature dependence of strain rate at 2500 psi is shown in figure 12. Although the apparent activation energy for densification decreases in a regular manner from 122 Kcal/mole at 0.25 porosity to 88 Kcal/mole at 0.02 porosity, the data were insufficient to establish this as a real interaction.

Above 1350° C the decrease in apparent activation energy at 2500 psi would suggest change in the primary mechanism controlling densification. This suggestion is supported by the fact that the apparent activation energy for densification between 1350° and 1450° C was also found to be stress dependent (fig. 13) and decreased from approximately 90 Kcal/mole at 867 psi to approximately 40 Kcal/mole at 5100 psi.

Multiple linear regression.— To determine the best values for the coefficients of the independent variables, the densification data in the low porosity regime ($P \leq 0.15$) were fitted (method of least squares) to a linear regression equation:

$$\log \dot{\epsilon} = b_0 + m \log P + n \log \sigma - 0.4343 \frac{Q}{R} \left(\frac{1}{T} \right) \quad (10)$$

Because of the changing character of densification above 1390° C, the data at 1450° C were excluded from the regression. The calculated coefficients and their associated 95 percent confidence intervals were as follows:

$$b_0 = 6.98$$

$$m = 1.20 \pm 0.05$$

$$n = 1.05 \pm 0.10$$

$$Q \text{ (Kcal/mole)} = 87.5 \pm 3.2$$

An analysis of variance for the multiple regression indicated that the chosen variables were highly significant and that more than 95 percent of the observed strain rate variance was explained by the regression.

The coefficients for porosity and stress (m and n) were used to determine a densification rate constant, K, as follows:

$$\log K = \log \dot{\epsilon} - m \log P - n \log \sigma \quad (11)$$

The temperature dependence of K is presented as an Arrhenius plot in figure 14. In this figure, the average of K was determined between 1260° and 1390° C for all applied stresses using the calculated values for m and n. The data at 1450° C are shown for stresses of 867, 1500 and 2500 psi. This figure in conjunction with the previous discussion of strain rate dependence on porosity and stress, clearly demonstrates the empirical independence of porosity suggested by the rate equation below 1390° C. The results (m > 1) also indicate that the consideration of porosity solely as a stress modifier may be overly restrictive. The calculated values of K at 1450° C are also consistent with the decrease in the apparent activation energy previously discussed for densification as a function of stress at stresses below the transition in strain rate-stress dependency.

Densification Mechanisms

In this section the primary mechanisms thought to be operative during the densification of magnesium aluminate by hot-pressing are qualitatively discussed. While the mechanisms proposed are by no means considered conclusive, they are supported by the experimental evidence of this investigation.

At temperatures below 1350° C the densification behavior is similar to other oxide ceramics; i.e., an initial region of rapid densification followed by a slower final process. The sharp change in the porosity dependence of strain rate observed at $P \approx 0.15$ separates these regions and is consistent with the geometrical restrictions on plastic flow at grain contacts which have been discussed by Coble and Ellis (ref. 24). Although a grain-size dependency was not established, the viscous behavior of the compacts and the lack of an end-point porosity were both in general agreement with the Nabarro-Herring diffusional creep mechanism.

The following indicate that the lack of linearity observed in the log porosity - time plot (fig. 1) above 1300° C was probably due to the effects of grain growth rather than a change in the mechanism or mechanisms controlling densification:

1. The lack of a stress-porosity interaction.
2. No change in the stress or temperature dependence of strain rate.
3. Agreement with the hyperbolic rate equation.

This hypothesis lends further support to the suggestion that densification was controlled by a diffusional creep mechanism since the Murray plastic flow model (ref. 1) does not suggest a grain size dependency.

At 1450° C the following suggest a transition in the primary densification mechanism to one involving plastic flow:

1. An interaction between stress and porosity.
2. An increase in the strain rate dependence on stress.
3. A stress sensitive apparent activation energy.

The strain rate-stress dependence ($\dot{\epsilon} \approx \sigma^4$) at the higher stresses suggests a plastic flow mechanism in agreement with the Weertman relation. Since this model is also based on a diffusionally controlled process (climb of dislocations), a change in the ionic species controlling the final stages of densification is necessary to resolve the conflict. This apparent conflict may be explained by: (1) the ionic species which control bulk diffusion (presumably one of the cations) and dislocation motion are different; (2) the change is the result of a deviation from stoichiometry. The first possibility can be supported by referring to the evidence for alumina which suggests cation control for bulk diffusion processes (see, for example, refs. 4 and 25) and anion control for dislocation motion (refs. 26 and 27). The second possibility may be the result of the reduction which occurs when spinel is hot-pressed in graphite dies (ref. 6). Similar deviations in stoichiometry and a change in the apparent activation energy have been observed in the creep behavior of rutile (ref. 28). The linear dependence of strain rate on stress and the stress sensitivity of the apparent activation energy provide support for the Peierls-Nabarro mechanism during the transition (ref. 27).

CONCLUSIONS

An investigation was made to characterize the densification behavior of magnesium aluminate during vacuum hot-pressing and to examine the applicability of a phenomenological rate equation. The following conclusions are made for the results presented herein:

1. The densification kinetics observed below 1450° C can be represented by the following rate equation:

$$\dot{\epsilon} = (9.53 \times 10^6) P^{1.20} \sigma^{1.05} \exp\left(\frac{-87,500}{RT}\right)$$

for values of porosity ≤ 0.15 .

2. At constant temperature the strain rate dependence on porosity increased for $P > 0.15$.

3. For temperatures between 1200° and 1350° C the densification characteristics of magnesium aluminate are similar to those reported for other oxide systems.

4. At 1350° C and above neither diffusional creep models nor plastic flow models adequately described the densification behavior observed. Between 1350° and 1450° C the apparent activation energy for densification was found to be stress dependent. At 1450° C an increase in the stress dependence of the densification rate and an interaction between stress and porosity indicated that plastic flow by dislocation motion was probably an operative mechanism during densification.

5. High densification rates at 1450° C for stresses of 2500 psi and above appeared to inhibit complete densification, possibly because of pore entrapment.

6. At 1350° C under an applied stress of 2500 psi, magnesium aluminate (approximately 98.5 percent pure) can be vacuum hot-pressed to 99.5 percent of theoretical density in approximately two hours.

REFERENCES

1. Murray, P.; Livey, D. T.; and Williams, J.: The Hot-Pressing of Ceramics. In W. D. Kingery (ed.), Ceramic Fabrication Processes. The Technology Press of M.I.T. and John Wiley and Sons, Inc., New York, 1958, pp. 147-170.
2. McClelland, J. D.: Kinetics of Hot-Pressing of Ceramics. In W. Leszynski (ed.) Powder Metallurgy - Proceedings of International Conference, New York, 1960. Interscience Publishers, New York, 1961, pp. 157-171.
3. Vasilos, T.; and Spriggs, R. M.: Pressure Sintering Mechanisms and Microstructures. J. Am. Ceram. Soc., Vol. 46, No. 10, 1963, pp. 493-496.
4. Rossi, R. C.; and Fulrath, R. M.: Final Stage Densification in Vacuum Hot-Pressing of Alumina. J. Am. Ceram. Soc., Vol. 48, No. 11, 1965, pp. 558-564.
5. Kovaltschenko, M. S.; and Samsonov, G. V.: Application of the Theory of Viscous Flow to the Sintering of Powders by Hot-Pressing. Poroschkovaja Metallurgia, Vol. 1, No. 2, 1961, pp. 3-13.
6. Kriegel, W. W.; Palmour, H., III; and Choi, D. M.: The Preparation and Mechanical Properties of Spinel. In P. Popper (ed.) Special Ceramics, 1964: Proceedings of a conference held at British Ceramic Research, Stoke on Trent. Academic Press, London, 1965, pp. 167-186.
7. Bakker, W. T.; and Lindsay, J. G.: Preparation and Properties of Reactive Magnesia Spinel. Rep. AS-6-66-17, Aluminum Res. Labs., Ltd., Aluminum Co. of Canada, June 1966.
8. Vasilos, T.: Hot-Pressing of Fused Silica. J. Am. Ceram. Soc., Vol. 43, No. 10, 1960, pp. 517-519.
9. Mangsen, G. E.; Lamberton, W. A.; and Best, B.: Hot-Pressing of Aluminum Oxide. J. Am. Ceram. Soc., Vol. 43, No. 2, 1960, pp. 55-59.
10. Jaeger, R. E.; and Egerton, L.: Hot-Pressing of Potassium-Sodium Niobates. J. Am. Ceram. Soc., Vol. 45, No. 5, 1962, pp. 209-213.
11. Kingery, W. D.; Woolbrown, J. M.; and Charvat, F. R.: Effects of Applied Pressure on Densification During Sintering in the Presence of a Liquid Phase. J. Am. Ceram. Soc., Vol. 46, No. 8, 1963, pp. 391-395.

12. Nabarro, F. R. N.: Deformation of Crystals by Motion of Single Ions. Report on a conference on Strength of Solids. Physical Society of London, 1948, pp. 75-90.
13. Herring, C.: Diffusional Viscosity of a Polycrystalline Solid. J. Appl. Phys., Vol. 21, No. 5, 1950, pp. 437-445.
14. Scholz, S.: Some New Aspects of Hot Pressing of Refractories, Special Ceramics 1962. Proc. Symp. by Brit. Ceram. Res. Assoc., Academic Press, New York, N. Y., 1962, pp. 293-307.
15. Carlson, R. G.; and Westermann, F. E.: Hot Pressing of Lead Spheres, Planseeber. Pulvermetallurgie, Vol. 10, 1962, pp. 15-23.
16. Scholz, S.: The Density-Time Relation in Hot Pressing, Planseeber. Pulvermetallurgie, Vol. 11, 1963, pp. 82-84.
17. Brown, S. D.; Biddulph, R. B.; and Wilcox, P. D.: A Strength-Porosity Relation Involving Different Pore Geometry and Orientation. J. Am. Ceram. Soc., Vol. 47, No. 7, 1964, pp. 320-322.
18. Knudsen, F. P.: Dependence of Mechanical Strength of Polycrystalline Specimens on Porosity and Grain Size. J. Am. Ceram. Soc., Vol. 42, No. 8, 1959, pp. 376-387.
19. Sherby, O. B.: Factors Affecting the High Temperature Strength of Crystalline Solids. Acta Metallurgica, Vol. 10, 1962, pp. 135-147.
20. Weertman, J. R.: Steady-State Creep Through Dislocation Climb. J. Appl. Phys., Vol. 28, 1957, pp. 362-364.
21. Choi, D. M.: Flow and Fracture of Hot-Pressured Polycrystalline Spinel at Elevated Temperatures. Ph.D. Thesis, Dept. of Mineral Industries, North Carolina State University, Raleigh. (Univ. Microfilm Service, Ann Arbor, Mich.), 1965.
22. McBrayer, R. D.: High Temperature Deformation of Alumina-Rich Spinel Single Crystals in Compression. Unpublished Ph.D. Thesis, Dept. of Mineral Industries, North Carolina State University, Raleigh. (Univ. Microfilm Service, Ann Arbor, Mich.), 1965.
23. Palmour, H., III: Multiple Slip Process in Magnesium Aluminate at High Temperatures. Presented at conference on Mechanical Properties of Nonmetallic Crystals and Polycrystals, April 5-7, 1965, Univ. of Birmingham, England. To be published in transactions no. 6 (in press).
24. Coble, R. L.; and Ellis, J. S.: Hot-Pressing Alumina - Mechanisms of Material Transport. J. Am. Ceram. Soc., Vol. 46, No. 9, Sept. 1963, pp. 438-441.

25. Chang, R.: Diffusion-Controlled Deformation and Shape Changes in Nonfissionable Ceramics. In A. Boltax and J. H. Handmerk (eds.) Nuclear Applications of Nonfissionable Ceramics, Proceedings of a conference held at Washington, D. C., May 1966, pp. 101-112.
26. Passmore, E.; Moschetti, A.; and Vasilos, T.: The Brittle-Ductile Transition in Polycrystalline Aluminum Oxide. Phil. Mag., Vol. 13, No. 126, June 1966, pp. 1157-1162.
27. Conrad, Hans: Mechanical Behavior of Sapphire. J. Am. Ceram. Soc., Vol. 48, No. 4, April 1965, pp. 195-201.
28. Hirthe, W. M.; and Brittain, J. O.: High-Temperature Steady-State Creep in Rutile. J. Am. Ceram. Soc., Vol. 46, No. 9, Sept. 1963, pp. 411-417.

TABLE I.- FABRICATION PARAMETERS, BULK DENSITY, POROSITY, AND RESULTS OF LINEAR REGRESSION ($\log \dot{\epsilon} = \log C + m \log P$) FOR MAGNESIUM ALUMINATE COMPACTS

Compact number (a)	Test temperature, °C	Applied stress, psi	Time to temperature, min	Press time, min	Bulk density, g/cm ³	Porosity (b)	Log C	m	Correlation coefficient	Regression, degrees of freedom	Calculated porosity	
											$\dot{\epsilon} = 1 \times 10^{-4}$, min ⁻¹	$\dot{\epsilon} = 1 \times 10^{-2}$, min ⁻¹
1	1174	2500	21	405	2.712	0.2434	2.35	10.40	0.957	15	0.2450	0.3814
2	1200	500	30	30	2.308	.3560	3.77	14.78	.971	15	.2978	.4067
3	1220	500	33	60	2.379	.3362	2.85	12.68	.966	23	.2880	.4141
4	1230	1000	35	61	2.488	.3058	1.13	8.09	.930	17	.2323	.4104
5	1200	1000	17	206	2.649	.2608	2.76	11.12	.976	25	.2467	.3733
6	1220	1040	21	399	2.847	.2057	.574	6.50	.970	22	.1981	.4022
7	1200	2000	32	60	2.667	.2559	.644	6.12	.962	20	.1742	.3698
8	1220	2500	21	300	3.095	.1364	-1.12	2.89	.951	12	.1005	.4947
9	1220	3000	34	60	2.684	.2511	.891	6.49	.971	16	.1765	.3587
10	1220	3000	27	120	2.875	.1978	.111	4.46	.970	29	.1343	.3772
11	1260	2500	23	340	3.459	.0348	----	----	----	---	----	----
12	1275	2500	19	359	3.534	.0139	-1.85	1.16	.960	24	.0139	.7455
13	1300	1040	19	241	3.379	.0572	----	----	----	---	----	----
14	1300	2500	19	219	3.546	.0106	-1.58	1.14	.992	13	.0073	.4242
15	1300	2500	21	300	3.554	.0083	-1.79	1.07	.986	7	.0086	.6413
16	1295	2500	19	336	3.561	.0065	-1.74	1.11	.986	19	.0091	.5363
17	1354	867	47	120	3.282	.0842	-1.65	1.37	.850	9	.0190	.5551
18	1360	867	20	278	3.490	.0264	-1.65	1.33	.992	11	.0172	.5428
19	1355	1500	31	120	3.477	.0299	-1.47	1.21	.943	18	.0081	.3676
20	1358	2500	17	22	3.321	.0734	-.63	1.57	.941	6	.0072	.1341
21	1350	2500	20	56	3.466	.0331	-1.03	1.32	.957	10	.0056	.1846
22	1354	2500	47	57	3.465	.0332	-1.56	.91	.909	9	.0021	.3297
23	1352	2500	31	60	3.446	.0385	-1.03	1.39	.979	14	.0073	.2012
24	1353	2500	18	120	3.541	.0121	-1.14	1.31	.976	19	.0065	.2201
25	1350	2500	19	123	3.552	.0089	-1.02	1.32	.992	12	.0056	.1808
26	1350	2500	20	120	3.543	.0115	-1.12	1.28	.992	10	.0057	.2052
27	1352	2500	32	120	3.529	.0154	-1.34	1.18	.978	17	.0056	.2783
28	1356	2500	24	180	3.574	.0029	-1.14	1.23	.985	14	.0047	.1985
29	1360	2500	17	278	3.577	.0020	-.88	1.38	.994	17	.0056	.1560
30	1360	3500	19	60	3.516	.0191	-1.02	1.23	.978	10	.0036	.1576
31	1352	3500	45	120	3.527	.0158	-1.47	1.11	.968	18	.0051	.3299
32	1360	5133	18	60	3.557	.0075	-1.01	1.09	.982	10	.0018	.1247
33	1360	5133	16	120	3.568	.0045	-.783	1.26	.957	18	.0023	.1077
34	1390	1460	21	292	3.570	.0040	-1.23	1.11	.987	13	.0031	.2025
35	1390	2500	21	111	3.567	.0047	-.113	1.04	.987	7	.0018	.1472
36	1390	2500	19	153	3.569	.0042	-.93	1.20	.979	6	.0028	.1286
37	1390	2500	21	157	3.568	.0045	-.901	1.29	.966	8	.0039	.1402
38	1465	867	19	120	3.561	.0064	-1.02	1.29	.990	12	.0048	.1719
39	1460	1500	22	120	3.569	.0042	-.70	1.39	.990	11	.0043	.1164
40	1450	2500	19	100	3.570	.0040	-.33	1.53	.968	15	.0040	.0816
41	1440	2500	17	120	3.569	.0042	.04	1.76	.959	11	.0051	.0699
42	1455	3500	25	60	3.573	.0031	-.03	1.50	.965	6	.0022	.0482
43	1448	3500	20	180	3.564	.0056	1.17	2.52	.971	8	.0089	.0553
44	1458	5133	20	120	3.572	.0033	1.60	2.44	.907	3	.0051	.0335

^aCompacts were not pressed in numbered sequence.

^bBased on pore free bulk density of 3.584g/cm³.

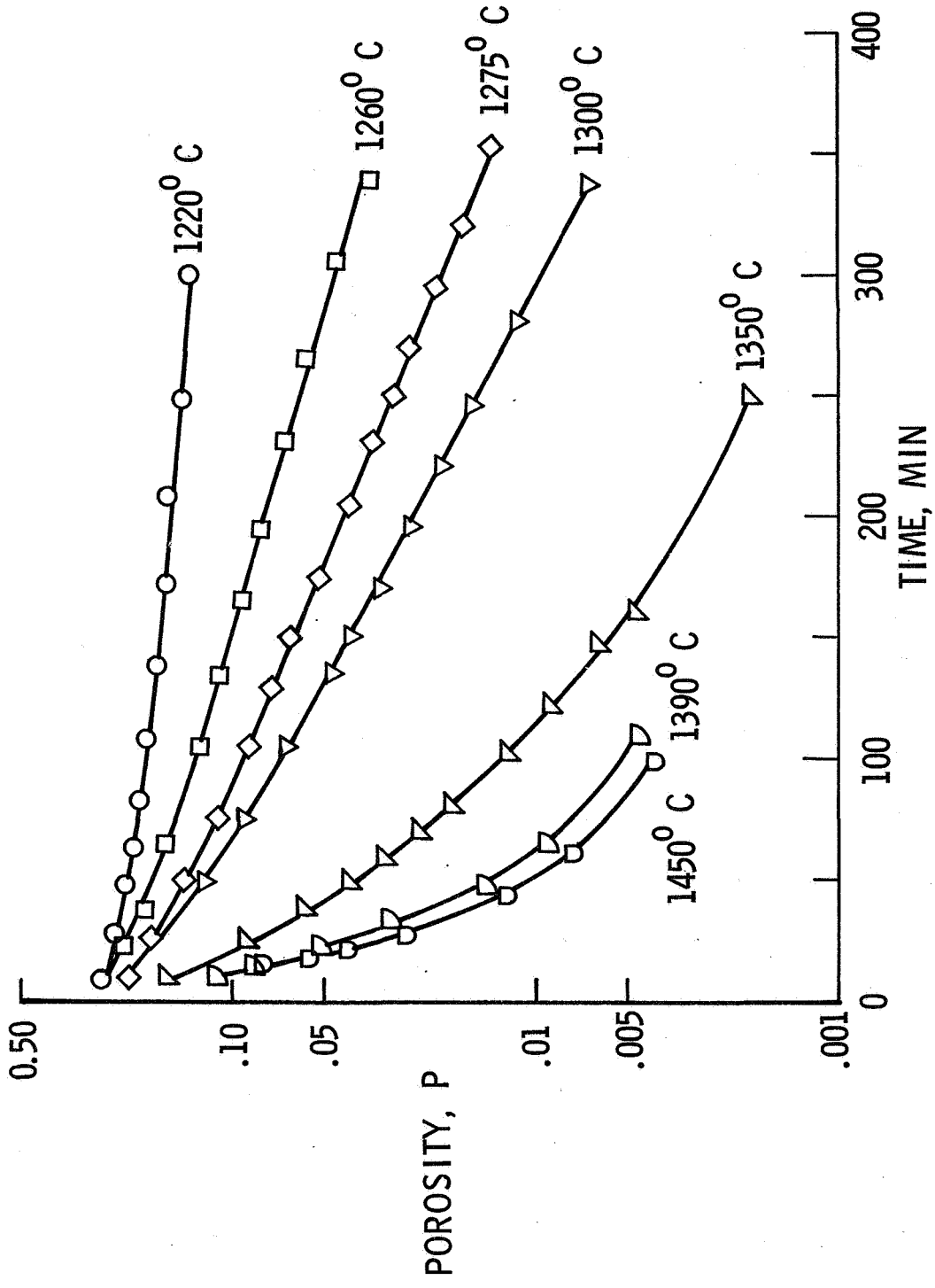


Figure 1.- Typical porosity dependence on time for spinel compacts at an applied stress of 2500 psi.

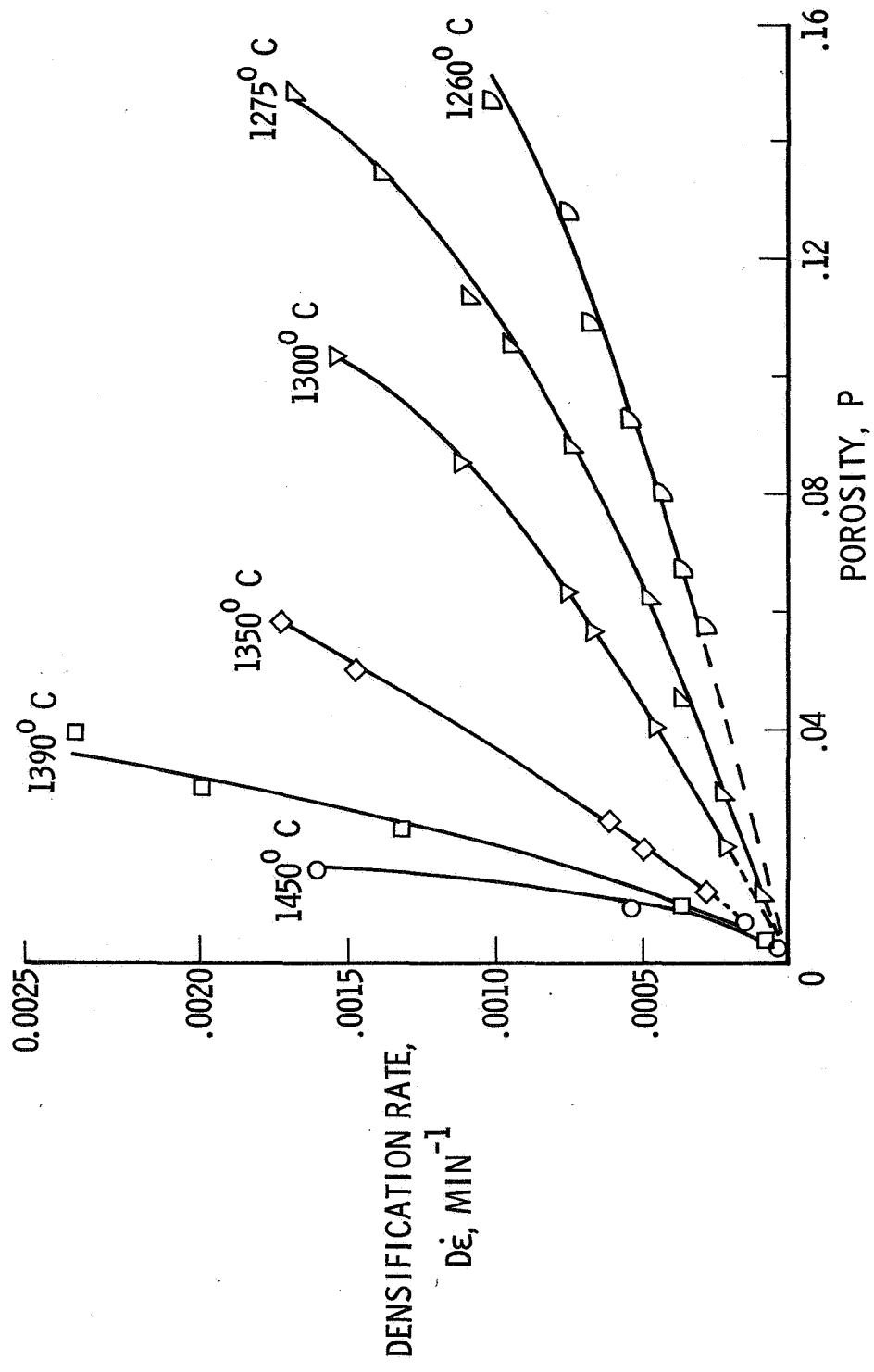


Figure 2.- Typical densification rate-porosity curves for spinel compacts at an applied stress of 2500 psi.

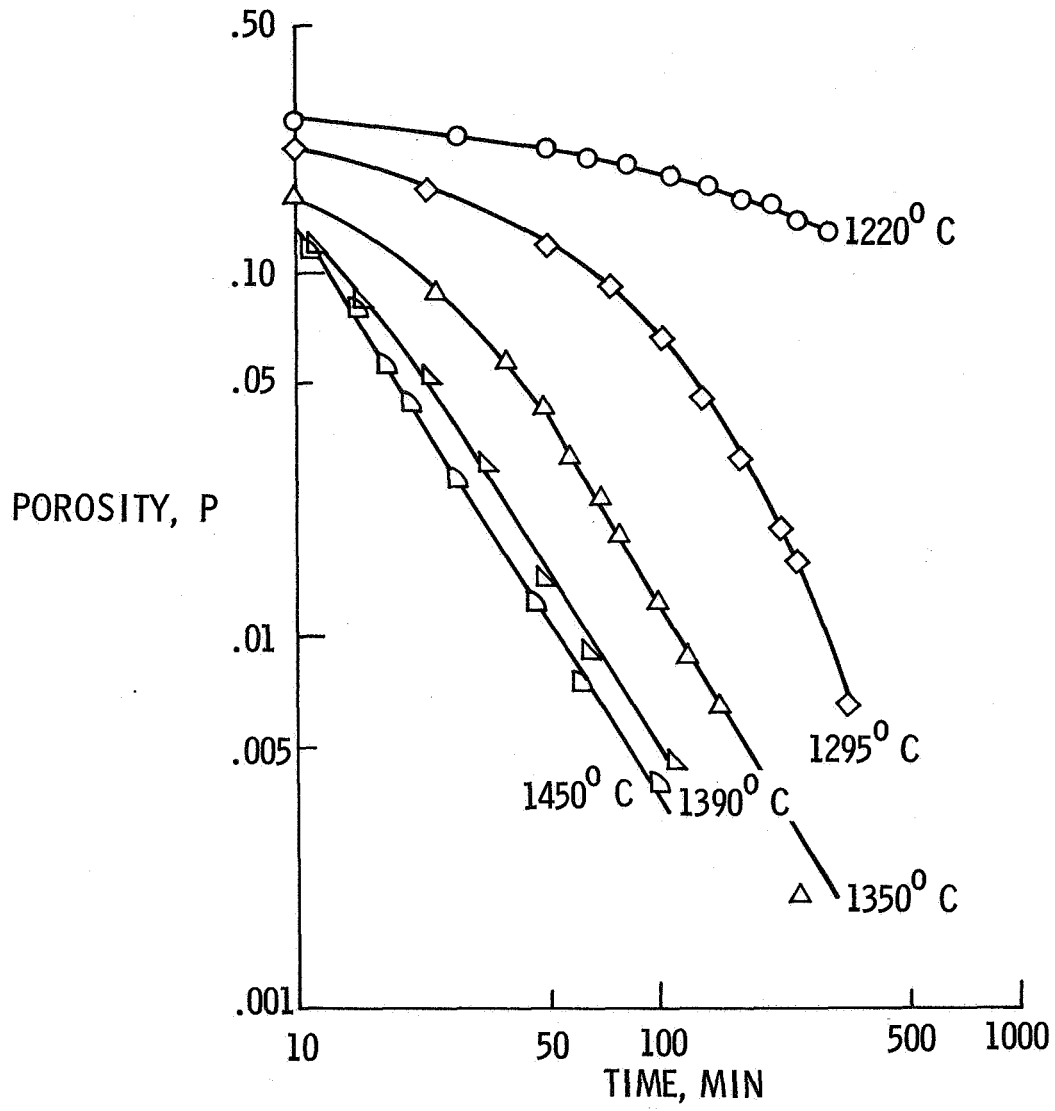


Figure 3.- Typical log porosity-log time behavior of spinel compacts at an applied stress of 2500 psi.

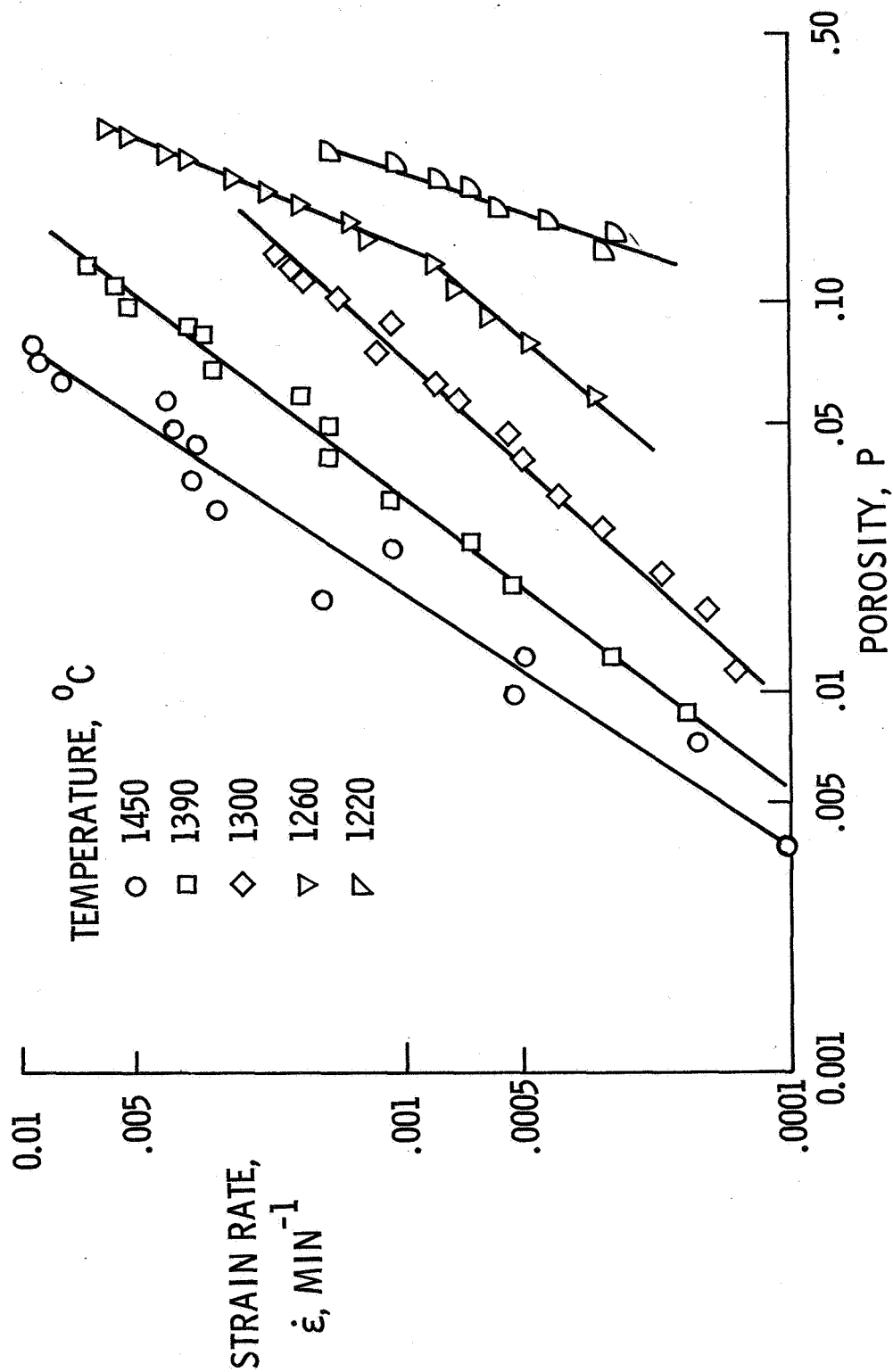


Figure 4.- Typical strain-rate dependence on porosity at an applied stress of 2500 psi for spinel compacts.

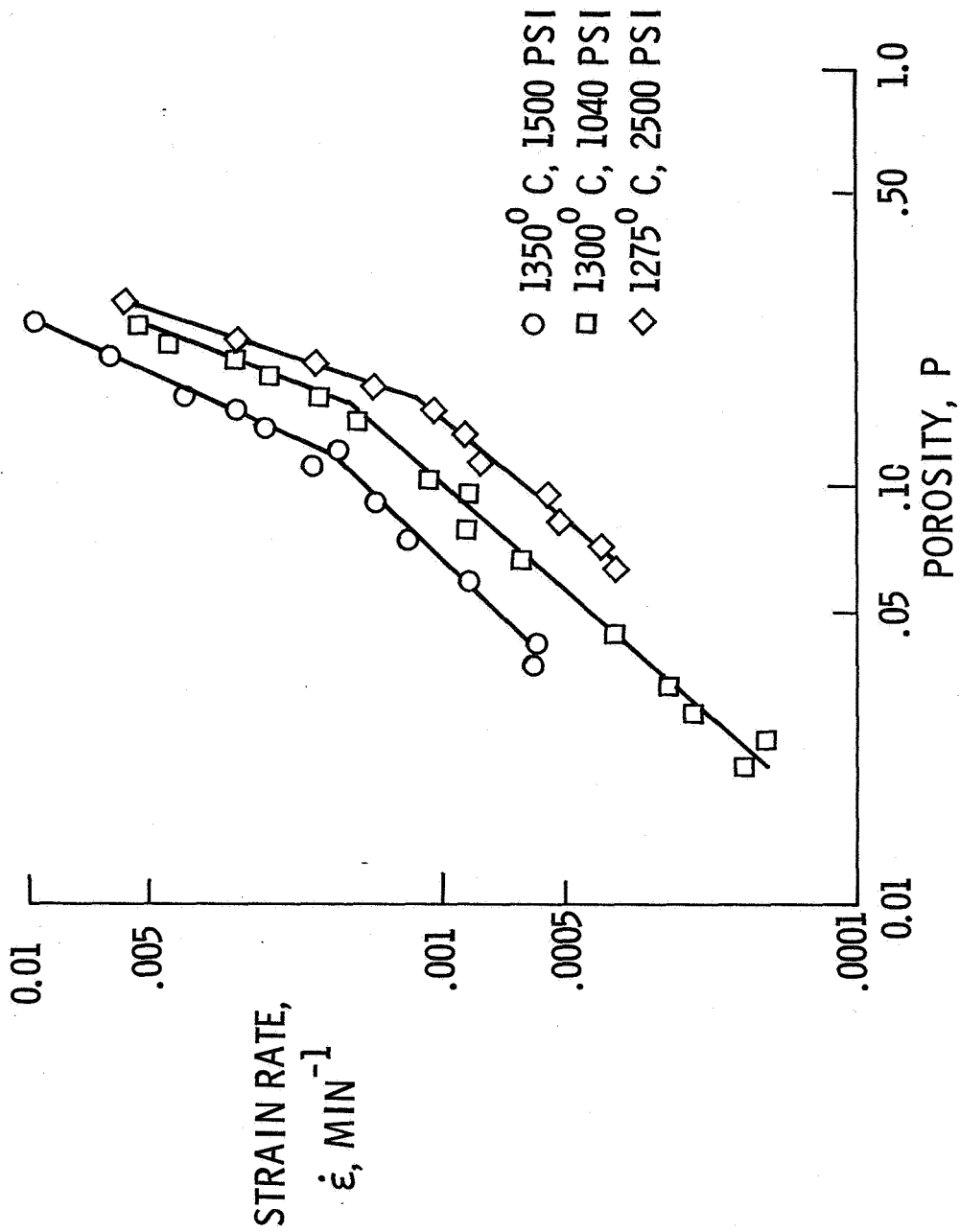


Figure 5.- Strain-rate dependence on porosity of spinel compacts for several combinations of temperature and stress.

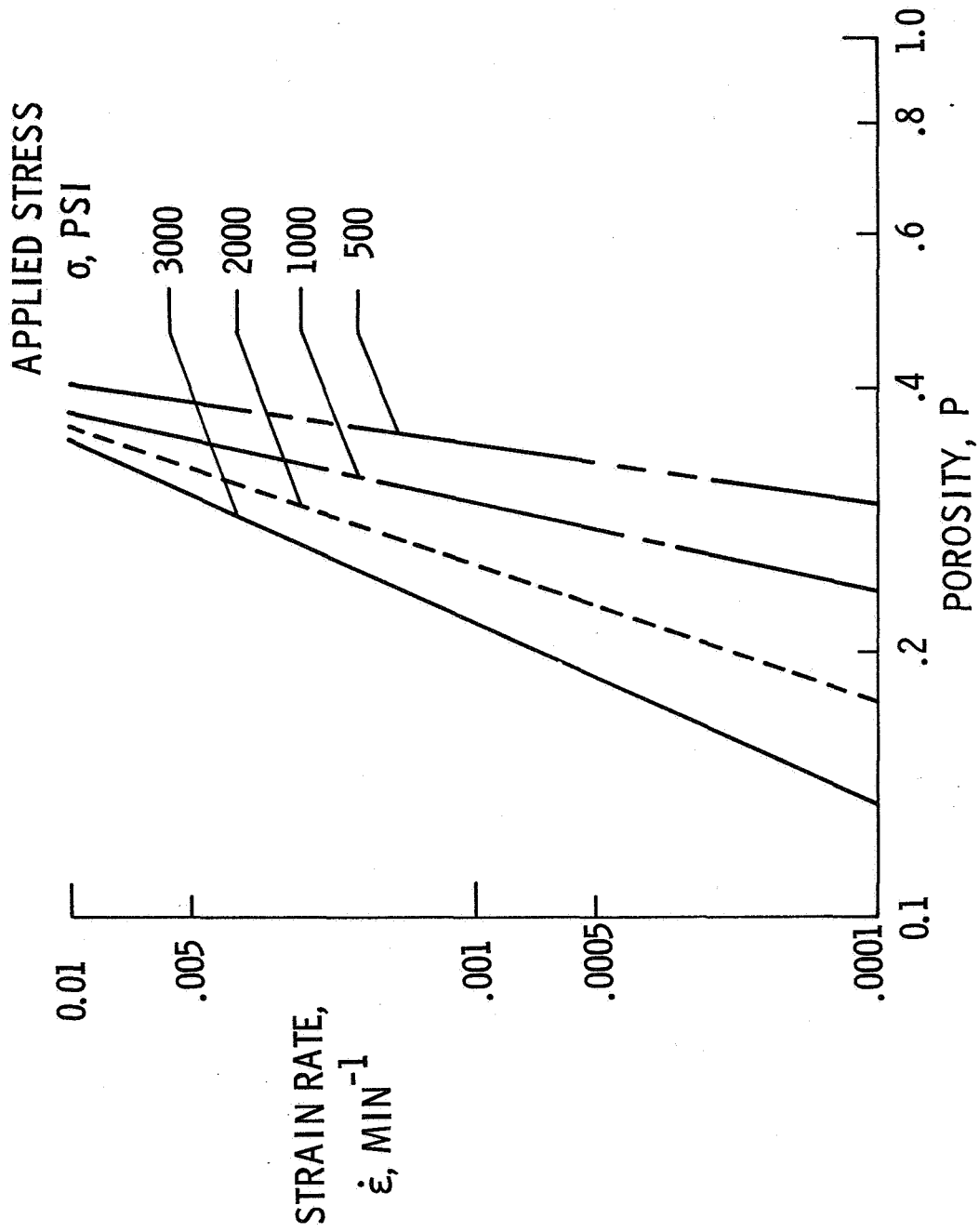


Figure 6.- Average regression lines for strain-rate dependence on porosity at 1220° C for spinel compacts.

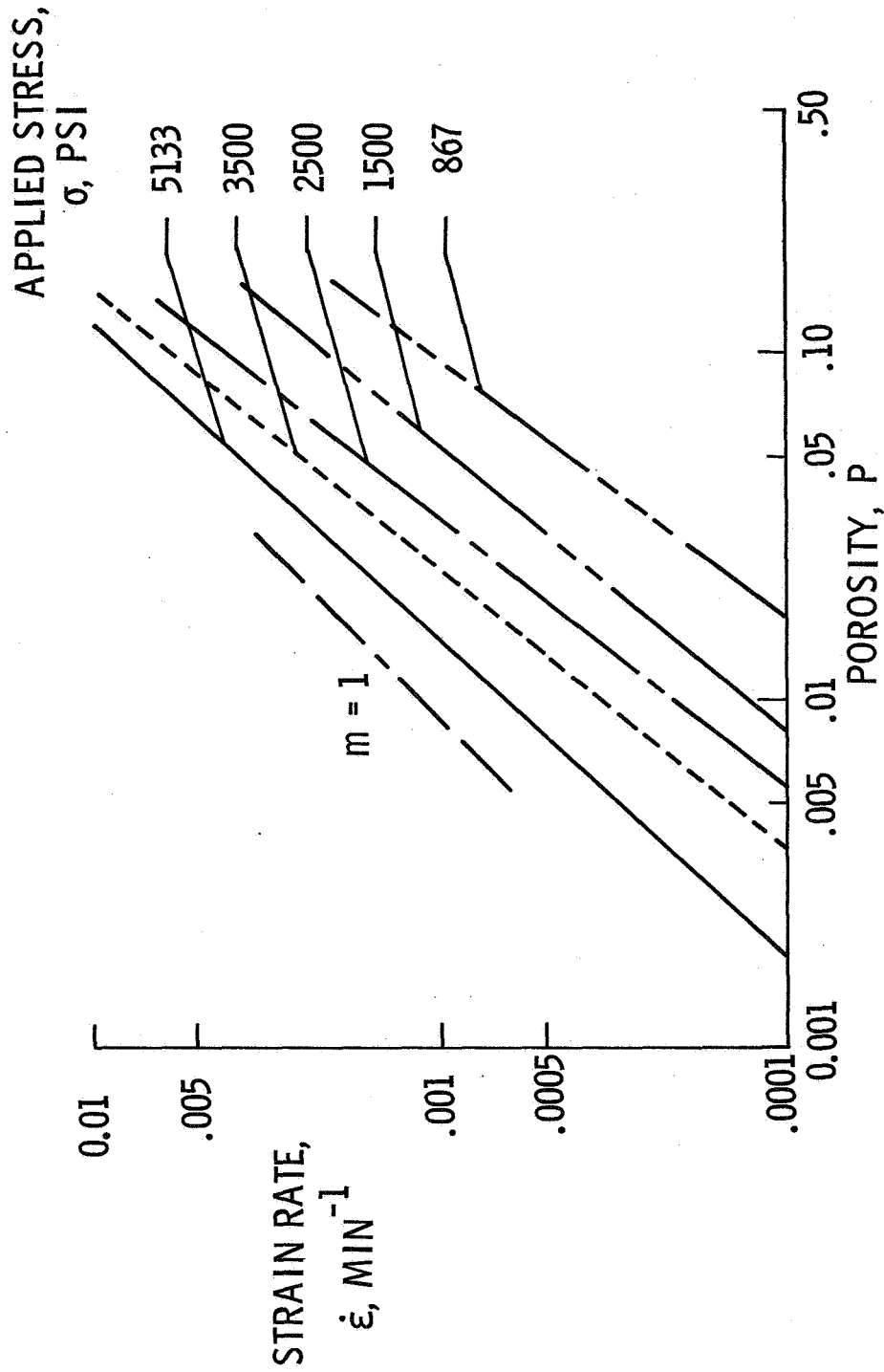


Figure 7.- Average regression lines for strain-rate dependence on porosity at 1350° C for spinel compacts.

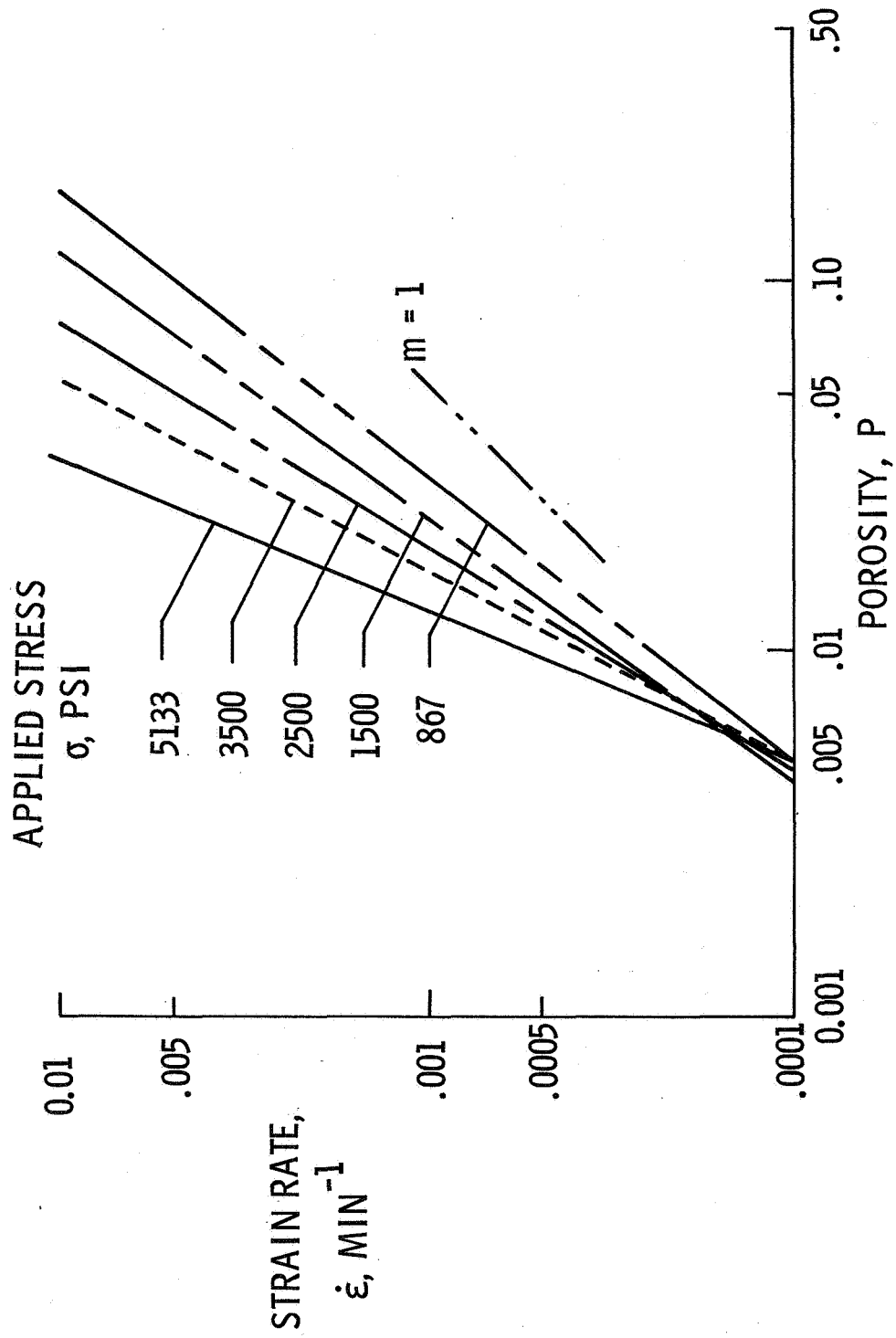


Figure 8.- Average regression lines for strain-rate dependence on porosity at 1450° C for spinel compacts.

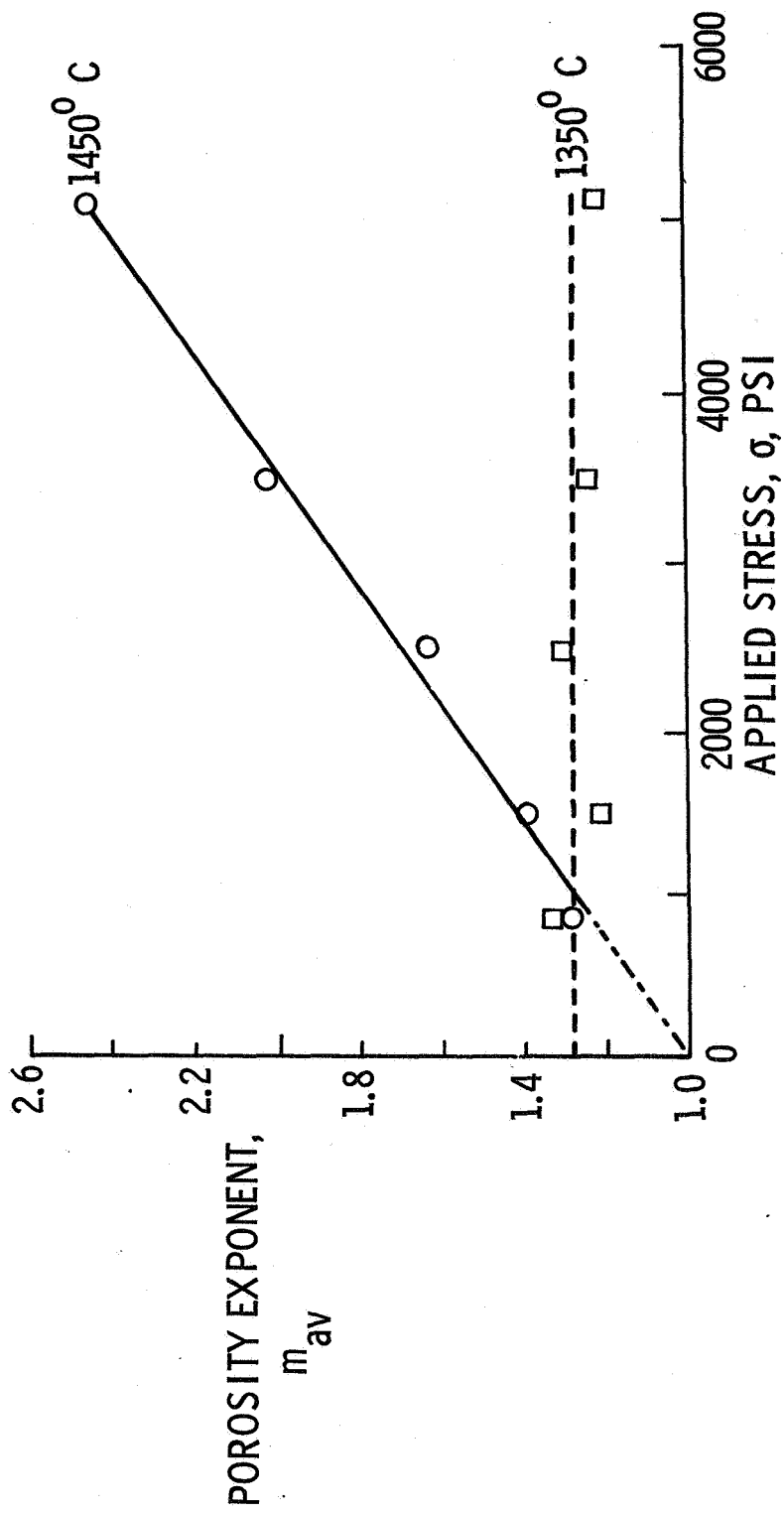


Figure 9.- Stress dependence of average porosity exponent for spinel compacts.

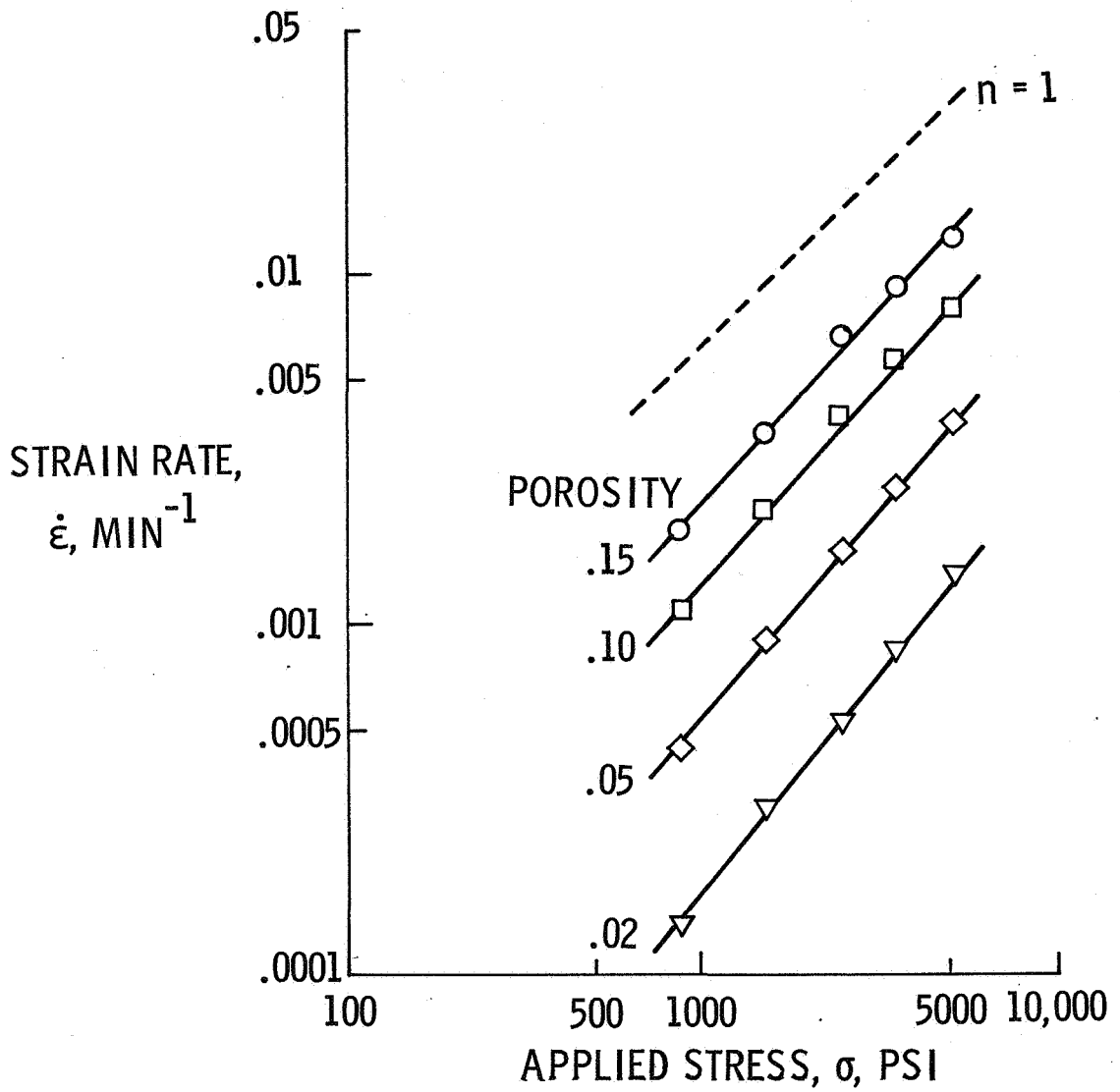


Figure 10.- Cross-plot of strain rate as a function of stress for spinel compacts at 1350°C .

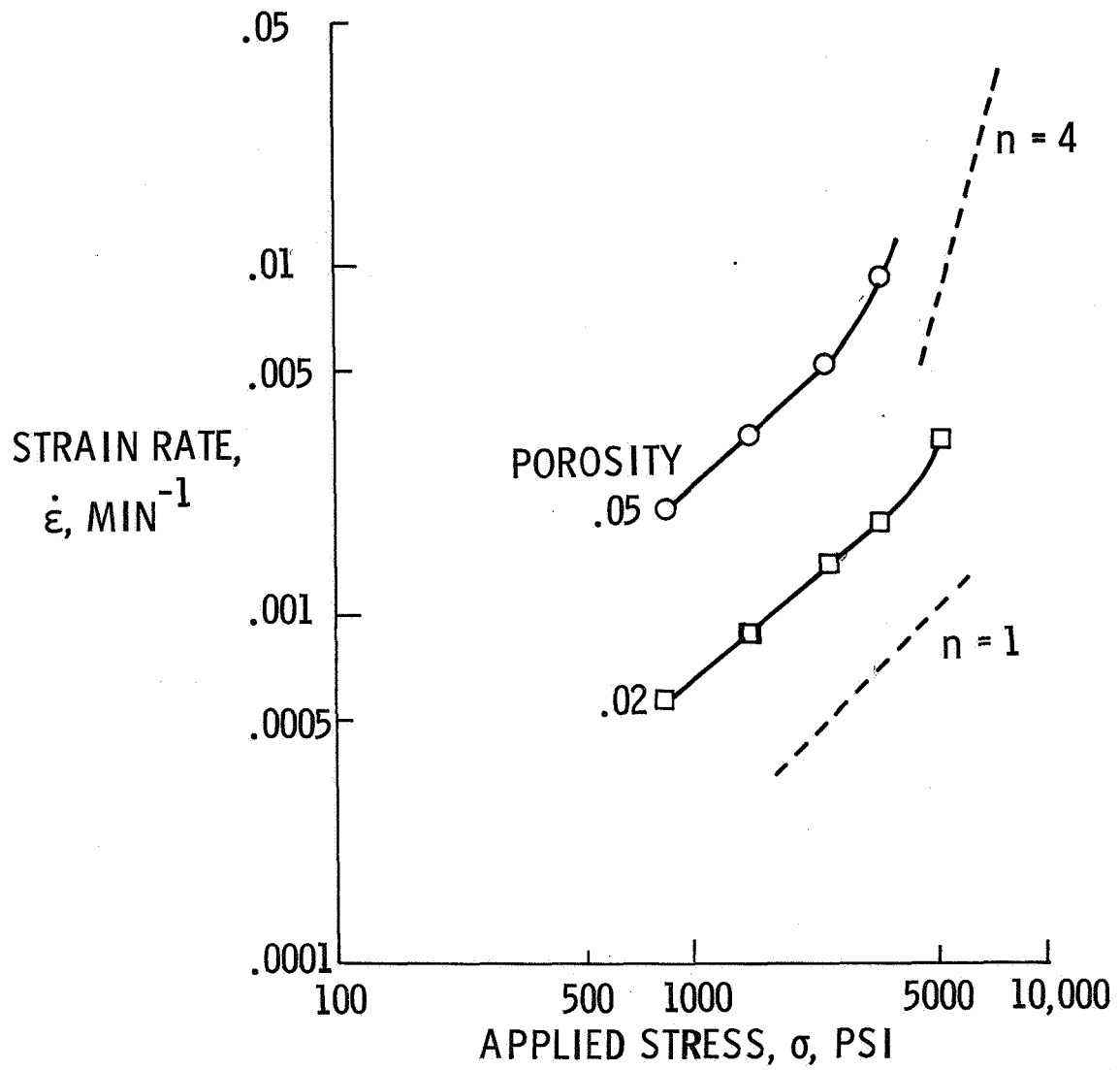


Figure 11.- Cross-plot of strain rate as a function of stress for spinel compacts at 1450° C.

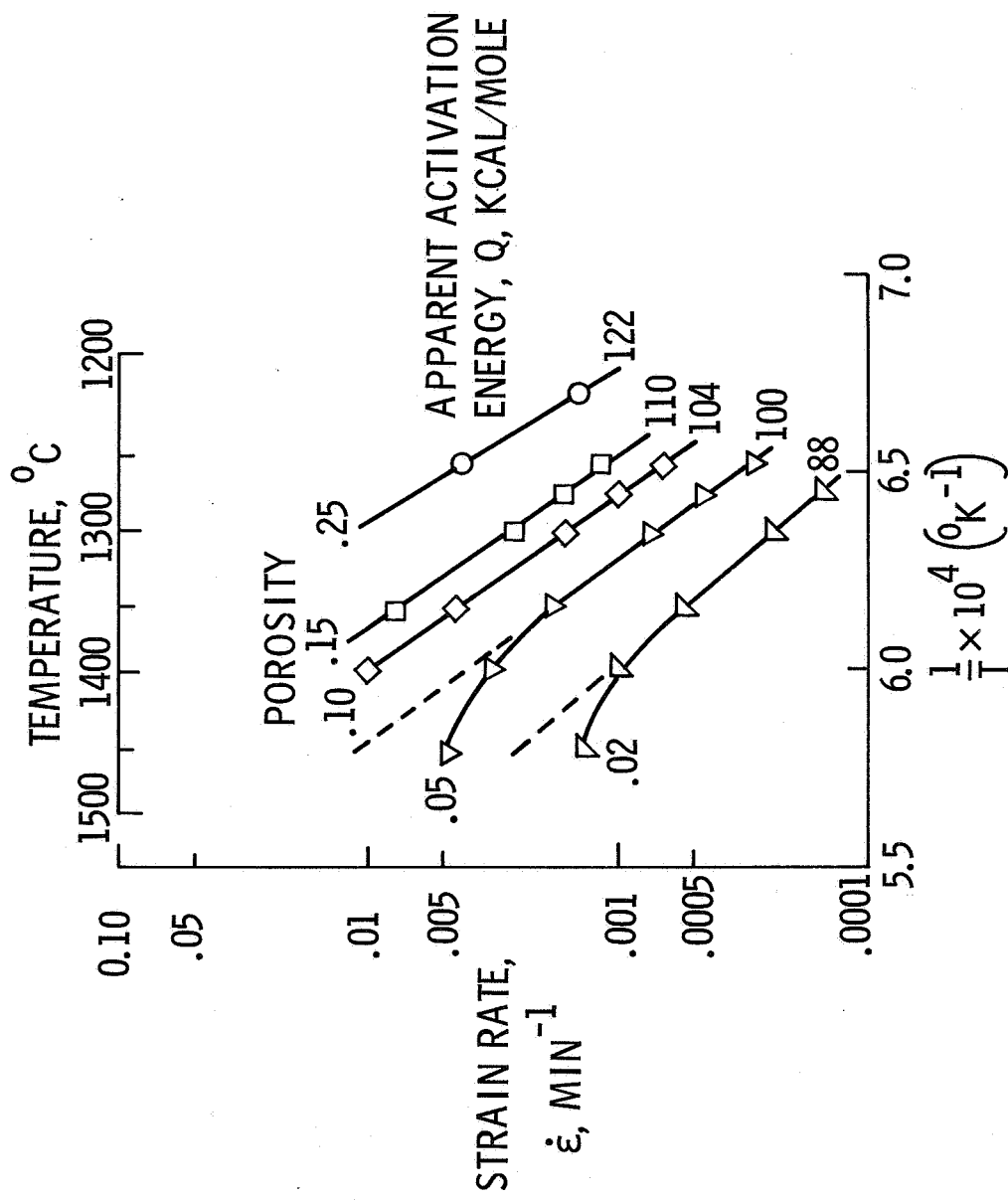


Figure 12.- Cross-plot of strain rate as a function of reciprocal temperature for spinel compacts at an applied stress of 2500 psi.

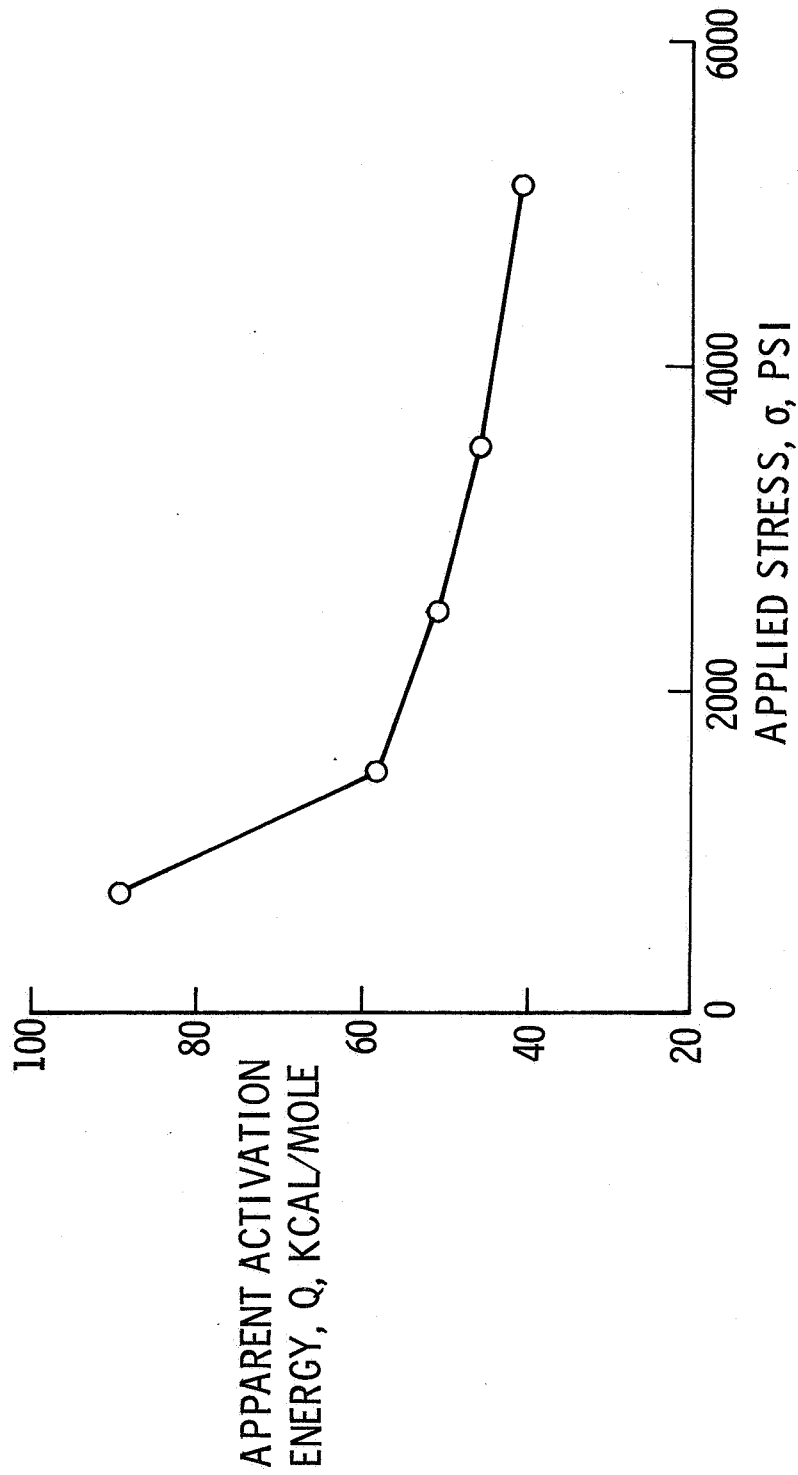


Figure 13.- Stress dependence of apparent activation energy at 2 percent porosity for spinel compacts between 1350° and 1450° C.

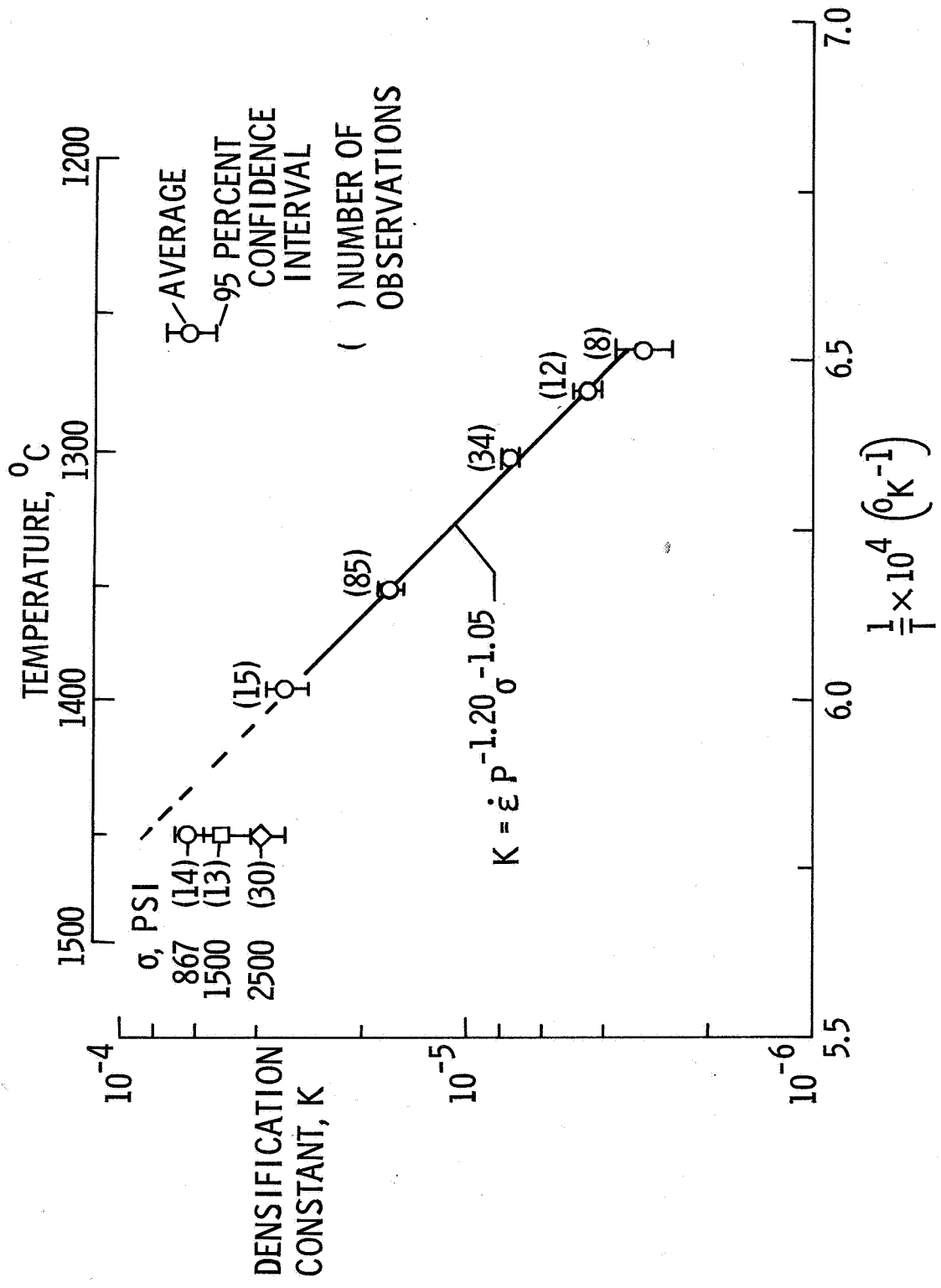


Figure 14.- Temperature dependence of densification constant, K.